Landslides (2005) 2:3–14
DOI 10.1007/s10346-004-0038-9
Received: 2 September 2004
Accepted: 20 October 2004
Published online: 13 January 2005

Laurent Tacher · Christophe Bonnard · Lyesse Laloui · Aurèle Parriaux

Modelling the behaviour of a large landslide with respect to hydrogeological and geomechanical parameter heterogeneity

Abstract Thanks to a sophisticated transient hydrogeological modelling allowing the determination of the pore pressure fields in La Frasse landslide mass during a crisis, it has been possible to model the mechanical behaviour of the slide and obtain results that prove to be similar to the monitored data, in terms of peak velocity, distribution of velocity with time and space and total displacements. Such results are reached only when appropriate constitutive modelling laws are used, and when geotechnical tests supply all the required parameters. The main results concern the potential effect of a drainage system during a crisis, like the one experienced in 1994. It can include vertical boreholes equipped with pumps or drains drilled from a gallery. The draining system reduces horizontal displacements down to 5% of the values modelled during the crisis. This effect, which appears to extend over a large width, will be even more significant if the boreholes discharge the drained water into the gallery, due to its extension in the presently stabilised landslide mass below the active zone. The modelling tools developed for La Frasse landslide thus provide all the necessary information to optimise the drainage scheme.

Introduction

Since its construction between 1836 and 1840, the major cantonal mountain road (RC 705) connecting the town of Aigle (El. 430 m a.s.l), to the village of Le Sépey (El. 1,000 m a.s.l.), and then leading to the Col des Mosses Pass (El. 1,445 m a.s.l.), has been regularly affected by significant displacements and occasional damage at the site where it crosses the La Frasse landslide (Fig. 1) (Prina et al. 2004). As this road is of strategic importance for the development of tourism, and experiences increasing traffic daily (5,000 vehicles/day in 1993), the Office of Roads and Motorways of the Canton of Vaud, in conjunction with the federal authorities, decided to investigate the possibility and reliability of various stabilisation schemes aiming at reducing the movement of this large slide, in particular through a drainage system.

Thus a joint venture was set up between several private consultants and two laboratories of the Swiss Federal Institute of Technology of Lausanne (EPFL), namely the Laboratory of Engineering and Environmental Geology and the Laboratory of Soil Mechanics, forming the "Association technique Norbert, De Cérenville Géotechnique + EPFL pour l'étude du glissement de La Frasse." It aims at developing modelling tools allowing the characterization of the behaviour of La Frasse landslide during crises, including the geological, hydrogeological and geomechanical aspects. This investigation, carried out between 2002 and 2003, has integrated all the results gathered by numerous previous studies undertaken by the members of this association (Bonnard 1984; Vulliet and Hutter 1988; Noverraz and Bonnard 1990; Association NCG + EPFL 2004).

Main features of La Frasse landslide

The La Frasse landslide extends over a length of 2,000 m whereas its width varies from 500 m in its upper and medium parts, to 1,000 m in its lower part, where it is eroded at its toe by the Grand-Eau River (Fig. 1). Its maximum depth varies from 50 m in the lower part to 110 m in the medium part, but the presently active slide extends down to depths of 40 and 80 m, respectively. Thus the volume of the active mass represents 42 million m^3 and the total landslide volume, including the stabilised zone below the active mass, reaches 73 million m^3, according the latest geological model. The total area, extending over more than 1 km^2, displays a slope of 11° in its upper part and of 20° in its lower part.

This slide, the movements of which can be quantified since 1868 thanks to the interpretation of ancient cadastral maps (Bonnard 1984), has experienced several crises in the past, especially in its lower part, in particular in 1910–1914, 1966, 1981–1982 and 1993–1994. These crises do not significantly affect its long-term behaviour in the upper and medium parts (except locally in 1966), in which the long-term average velocity varies from 10 to 15 cm/year, but are quite sensible in the lower part, in which the long-term average velocity, from 20 to 60 cm/year, may present displacements during crises of up to 4 m (maximum observed velocity of 1 m/week).

In depth, the numerous inclinometer readings confirm that most of the movements are concentrated on the main slip surface, whereas secondary superficial slides display an activity especially in the lower part (+ and ++ zones, Fig. 4). These shallow

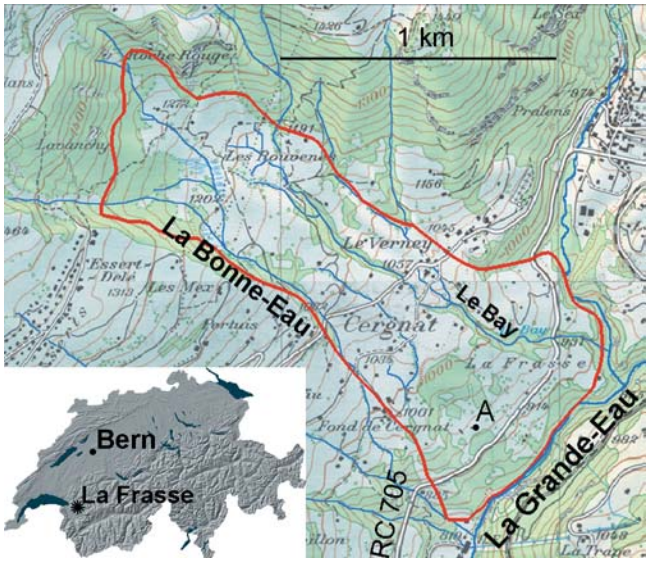

Fig. 1 Location of the La Frasse landslide. Point *A* refers to the caption of Fig. 5

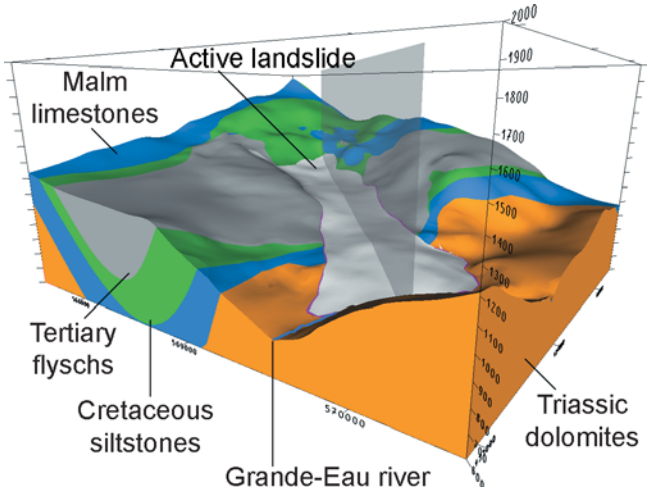

Fig. 2 Geological model and location of the vertical cross section. View from SE. Superficial moraine deposits were removed from the view

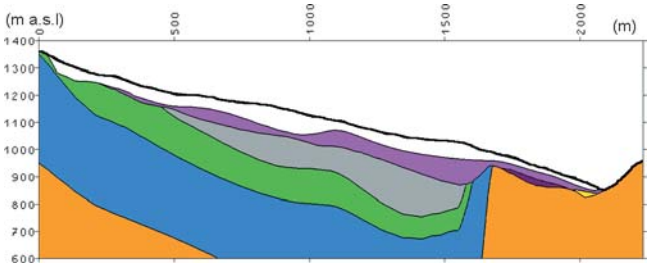

Fig. 3 Vertical cross section. Legend according Fig. 2; *purple* stabilised slide, *dark purple* moraine deposit, *yellow* former Grande-Eau River bed

movements were reduced first by the boring of a series of 10 m long anchored piles along the road in 1987, limiting its displacements to the movement component observed at the slip surface. A local pumping platform including 21 drainage boreholes was then carried out following the 1994 crisis (the commissioning of the drainage platform, the location of which is shown in Fig. 4, intervened in mid-December 1994, so that it is called the "1995 platform").

Since this period, the movements in the lower part of the slide have reduced significantly, either due to the natural velocity decrease generally observed after a crisis period, or due to the effect of the local groundwater drawdown. The data collected by this test drainage platform did supply significant data for the hydrogeological modelling.

Geological context

In accordance with the main alpine structures, La Frasse landslide is oriented NW to SE, down to the Grande-Eau River which erodes its toe continuously (Fig. 2). The regional geological structure is a pinched syncline of Mesozoic (Triassic dolomites, Malm limestones and upper Cretaceous siltstones) filled with the Tertiary flysch of the Simme nappe, which constitutes most of the sliding mass (Lugeon et al. 1922). At the end of the Würmian glaciation (14,000 years), the glacier covering the entire region retreated after having particularly eroded the Mesozoic substratum in La Frasse area, due to a set of local NW-SE faults. Thus, the obstacle

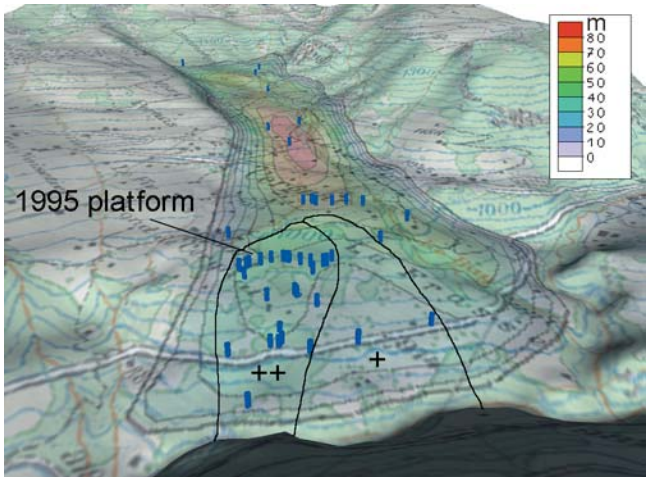

Fig. 4 Active landslide thickness, borehole location and most active areas (zones + and ++)

to the sliding of the flysch, created by the hard Malm flank of the reverse syncline, vanished.

A main sliding surface has been identified at a mean depth varying from 40 to 80 m, based on some 50 boreholes that were drilled between 1967 and 2002. Below this surface, a deeper flysch slide involving the flysch was identified by boreholes, which is at present stabilised (Fig. 3).

The flysch forming the main part of the sliding mass is made of sandstones and clay schists, consisting of strongly weathered to plastic black clay including sandy blocks. In addition, a large amount of Cretaceous siltstones and surface moraine fragments is included, respectively, in the upper and lower part of the mass. The initial heterogeneity of the flysch is thus increased by the landslide movements and the incorporation of other rocks, forming an extremely heterogeneous mass.

C^{14} dating of wood fragments shows that the landslide has been active for millennia. These data yield a mean velocity of about 7 cm/year at geological time scale, which is compatible with the available measurements covering the past two centuries (Bonnard 1984). This suggests a rather regular long-term behaviour. However, sliding velocities vary in space and time: in the upper part (NW), they range from some centimetres to decimetres per year; in the lower part, due to a reduced thickness of the sliding mass and its steeper slope, velocities are higher (e.g. during the 1981–1982 crisis, they locally reached 4 m with a maximum value of 1 m/week). The calcareous barrier, though eroded, constitutes a sill at the bottom of the slide, thus playing a part in its behaviour. Uphill, the topography presents a gentle slope approximately at El. 1000 m a.s.l; downhill, the fastest movements are observed. Thus, the Malm limestones and Triassic dolomites have a stabilising effect on the upstream part of the slide. Once overridden this obstacle, the slide materials do not meet any more hitches toward the Grande-Eau River, their acceleration being increased by a thinning of the sliding mass. Between El. 1000 m a.s.l. and the Grande-Eau, movements have also a lateral heterogeneity. In the SW, the long-term velocities are about 50 cm/year (++ zone, Fig. 4), decreasing to 20–30 cm/year in the median part (+ zone) and to 5–10 cm/year in the NE (average values before the commissioning of the 1995 pumping platform) (Noverraz and Bonnard 1990). This is related to the

longitudinal profile of the Grande-Eau River, the level of which loses approximately 40 m between its upstream and downstream contact with the slide, causing a higher topographic gradient toward the SW, although the river bed level has tended to rise during the last 50 years.

A 3-D structural geological model synthesizing all available data (boreholes, geophysics, field observations) has been built to design the stabilisation project. It supplies also the shape on which are based finite element meshes for hydrogeological and geomechanical numerical modelling

Hydrogeological characterization and modelling

Due to the high heterogeneity of the materials, the entire mass is considered as an aquifer at the scale of the slide. The correlation of borehole logs a dozen of meters apart is, in general, impossible. Local excess groundwater pressures are present not only at the main slip surface but also inside the sliding mass (e.g. borehole FR6, mentioned in Fig. 6, which showed two artesian levels at a depth of 18 and 42 m, the slip surface being at 51 m deep). This is why special care is paid to the characterization of hydrogeological conditions, even if the detail of the groundwater flows cannot be determined.

A first consequence of this situation is that in-depth drainage works should tend to drain both the flysch mass and the slip surface, which remains the place of preferential circulations. This local feature is probably due to the intense remoulding of the structure of the flysch and it has been observed by the pumping tests. A sustainable remediation solution must drawdown and stabilise hydraulic heads in the all thickness of the system. Therefore, a series of wells or sub vertical drains, located at the top of the most active part of the landslide (+ and ++ zones), drilled from a gallery in the substratum or from the surface, proves to be the most appropriate solution after an analysis of other possible designs. A second consequence of the heterogeneous character of the permeability field is that modelling investigations have to be addressed both at the landslide scale, in order to assess and understand the global behaviour, and at a local scale to design remediation structures.

Conceptual model

Infiltration conditions

Although groundwater is recognized to be the cause of the sliding, there is no clear relationship between the acceleration phases and either gross rainfall or net infiltration computed by simple formulas. Even the correlation of movements with accurately computed infiltration (COUP model, Jansson and Karlberg 2001) is poor.

However, a correlation has been found weighting the COUP infiltration data in the past and then considering only the daily values above a threshold value (truncation process). The weighting algorithm first consists in computing for each day the weighted sum of the infiltration according to two half Gaussian distributions, one with a small standard deviation (weighting by recent infiltration events) and one with a large standard deviation (weighting by seasonal and annual conditions). Then the computed sums below a certain threshold value are eliminated. A minimization process shows that the best correlation (Fig. 5) is obtained with standard deviations of 10 and 450 days, respectively, giving 85% of the total weight to the latter. As far as the

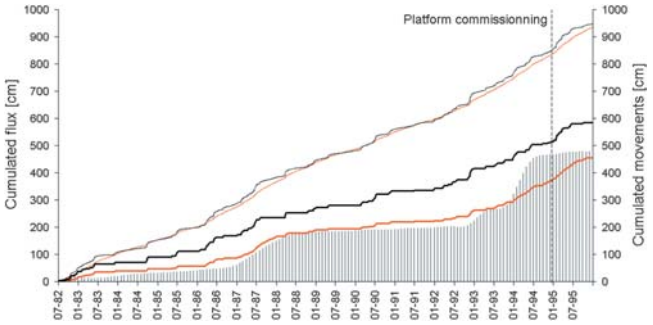

Fig. 5 Relationships between observed horizontal displacements at point A (Fig. 1) and computed flux entering the slide in a cumulated representation. *Thin black line* infiltration issued from COUP model (considering temperature, snowmelt, vegetation, soil, sun exposure...). *Thin orange line* weighted infiltration. *Thick black line* truncated infiltration. *Thick orange line* weighted and truncated infiltration. Note that due to the vertical scaling, the better fit of the thick orange curve with the displacements (*vertical bars*) is concluded from the shape of the curves rather than from the value of the corresponding points

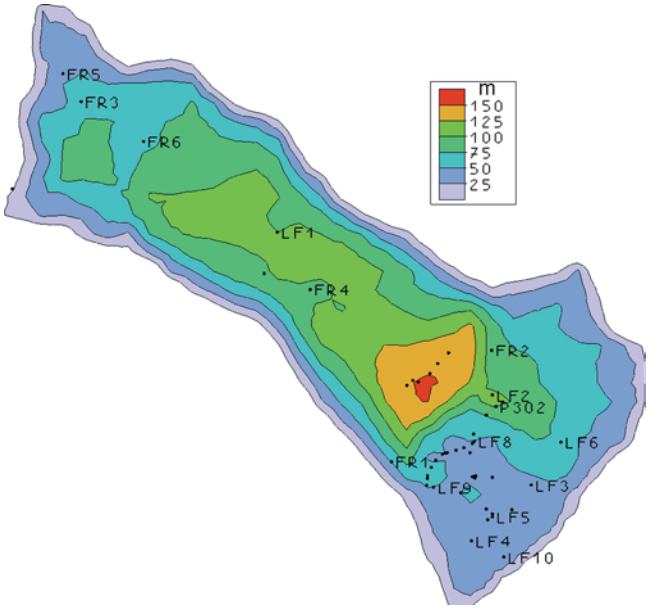

Fig. 6 Location of some representative boreholes and total thickness of the landslide mass (active plus stabilised). The maximum thickness occurs just uphill the syncline carbonates flank (Fig. 3)

threshold value is concerned, the best fit within the minimisation process is found with a truncated infiltration set to 1.9 mm/day.

For both Gaussian distributions, data untill 2 years before the computation day are considered. This means that rainfall events recorded in the past do intervene in the present behaviour of the landslide.

In detail, the in-situ flysch enclosing the landslide, due to its lithology and structure, has both a capacitive and conductive function. Field observation and deep boreholes show that the flysch layers are fractured, thus being able to quickly transfer an infiltration event to the sliding mass. This is the reason for considering a shorter standard deviation in the weighting process, which additionally represents the direct inflow from the landslide surface via the thin unsaturated zone. On the other hand, flysch is

also made of low permeability rocks able to store and to smooth out events far back in the past. This is represented by the long standard deviation term in the weighting process. The need for a threshold value to improve the correlation means that only the most important feeding events contribute to the increase of pore pressures and in turn to the sliding of the mass.

Since the long-term component is dominant, one must conclude that the slide is fed by the geological bodies enclosing it (mainly the in-situ flysch since carbonates are unsaturated over a large thickness) rather than by direct infiltration from the surface. Thus, a remediation scheme considering shallow drainage only is inappropriate and at least insufficient.

Furthermore, as the slide is surrounded by the adjacent in-situ flysch, the inflow comes through its lateral borders. Indeed, boreholes and a tracer test show that the hydraulic relationships of the slide with the underlying bedrock are weak, if existent, as shown by the following facts:

- Uphill, artesian levels in boreholes FR5 and FR6 are located within the sliding mass (Fig. 6). When reaching the substratum (stabilised landslide), the hydraulic head in the borehole remained unchanged. The FR3 borehole did not show important inflow, but reaching the Cretaceous siltstones, the hydraulic head dropped by about 5 m. In these three cases, the substratum does not feed the slide and even may tend to drain it.
- Downhill, P302, LF2, LF3, LF4, LF5, LF6 and LF8 boreholes became absorbent when reaching the karstic substratum (Trias and mainly Malm). This behaviour is due to the higher permeability of the karst, which works as a regional drain, as shown by the Chevrier tracer test (Parriaux et al. 1987). Indeed, the three piezometric sensors in borehole FR1 show a downward flux.
- The situation is less clear halfway up, at El. 1,100 m a.s.l. approximately. Inflows occur in borehole LF1 at a depth of 102 m, whereas the in-situ flysch was touched at 94.50 m. In borehole FR4, data are fragmentary but also show inflows in the in-situ flysch at the depth of 88 m. Thus, due to the total landslide thickening (active plus stabilised mass, as shown in Fig. 6), there is a possible tendency for a recharge by the substratum in this area, but it is impeded by the low permeability of the in-situ flysch (1E-7–1E-6 m/s).

An additional argument to this discussion leads to notice that the Bonne-Eau River (Fig. 1) springs from the landslide along its SW boundary and that the major part of its discharge is gained crossing the in-situ flysch.

For all these reasons, hydraulic exchanges between the bedrock and the landslide through its basement appear to be negligible and are not considered in the numerical model.

Outlets

Numerous springs are scattered over the landslide; their total rate is of the order of some litres per second, leading to a total of about 1,000 m^3/day. In the NW, a humid area occurs close to El. 1200 m a.s.l. About 1,000 m^3/day are also drained by the Bonne-Eau and Le Bay streams (locally and temporarily, gauging showed also local infiltrations). However, the hydraulic connection of all these outlets with the aquifer is doubtful since nearby boreholes show systematically that the aquifer is some meters below, mainly in the downward part of the landslide. Thus, springs correspond to very shallow local aquifers that influence the bulk hydraulic balance of the slide by reducing the direct infiltration through the surface.

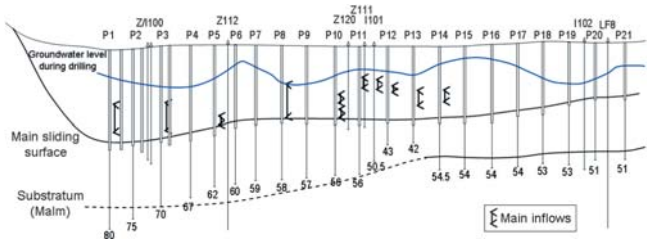

Fig. 7 Vertical cross section through the 1995 borehole platform. *Bottom value* depth of the boreholes (m)

The main outlet of the system is the Grande-Eau River; the discharge at the toe of the slide is estimated by means of balance computations at about 5,000 m^3/day.

Heterogeneity

The sliding process adds heterogeneity to the original one due to the flysch, leading to a network of more permeable structures (1.10^{-2} m/s or more) in a low permeability shale matrix (ca. 1.10^{-7} m/s), as it could be derived from a global interpretation of the hydrogeological data. Geological data issued from the 1995 platform investigations (Norbert and de Cérenville 1979) also show a high variability between boreholes spaced some 10 m apart (Fig. 7), which is considered as the width of the permeable structures. Originally, all 21 wells were designed to infiltrate water in the permeable carbonate substratum, but due to insufficient absorption capacity and depth of the carbonates, 18 of them had to be equipped with pumps.

Pumping tests carried out in 2002 and 2003 show that the connectivity of the permeable structures is higher in a direction parallel to the landslide and reaches hundreds of meters. Typically, stopping the 1995 pumping platform and restarting only the P11 pump 5 days later showed that piezometers Z203 and Z204 situated more than 200 m away reacted strongly (Fig. 8) whereas others much closer do not show any response.

Numerical models

The hydrogeological modelling using the Feflow software (Wasy AG 2004) consists in calculating the groundwater pressure field everywhere in the slide, which is then introduced at the slip surface at each time step into the geomechanical models. Several models were carried out to adequately represent the slide under natural conditions (without drainage) and then to assess the effect of the planned remediation works. The parameters (permeability k and specific storage S_s coefficients) and boundary conditions are initially tuned according to natural conditions. Once this calibration is obtained, boundary conditions specific to remediation scheme are added. For safety reasons, the parameters and boundary conditions were certainly selected in a reasonable range of values, but so that the prediction of the efficiency of the remediation works considered would be rather pessimistic. All the numerical hydrogeological models are built in 3-D in order to represent both the vertical and lateral heterogeneity of the parameters and boundary conditions. The pressure field is computed in a transient mode. However, in the models, physical parameters remain constant (e.g. no temporal change of the permeability field). The flow regime is saturated, which implies that

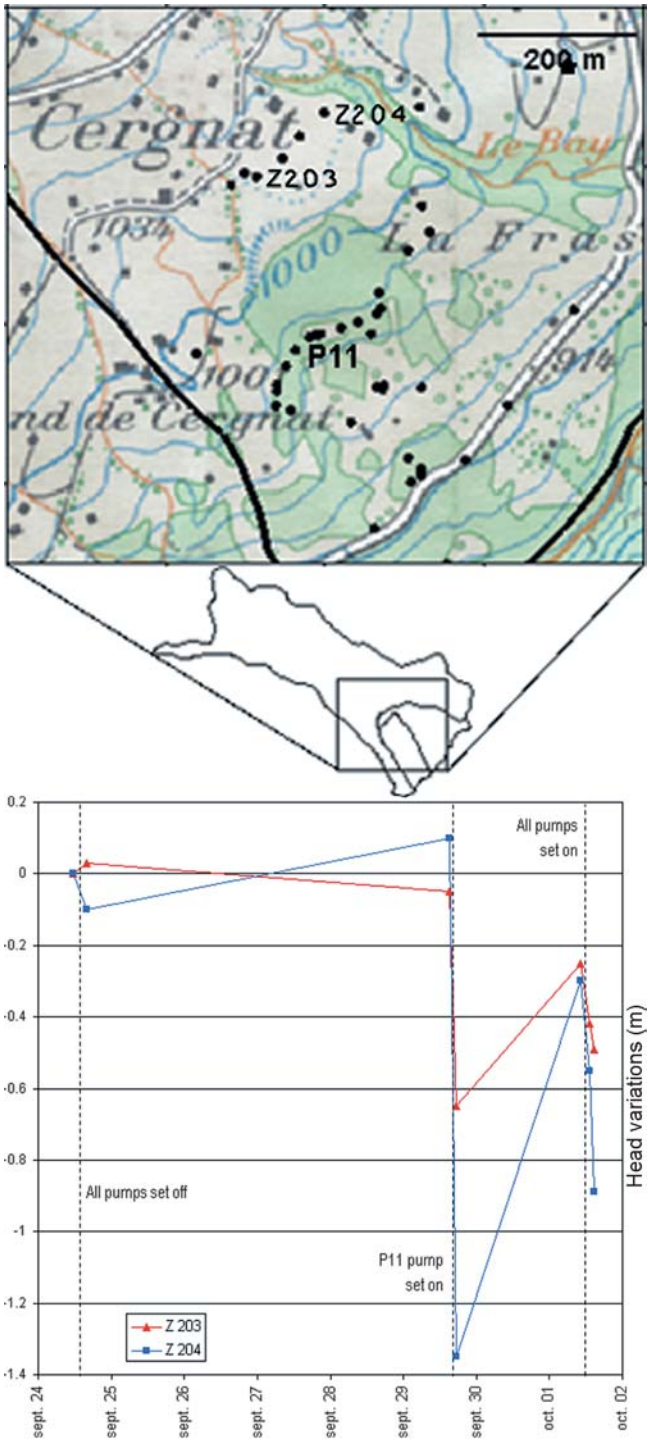

Fig. 8 Response of piezometers Z203 and Z204 to platform setting off (September 24, 2003) and setting on of well P11 (September 29, 2003)

the slide body is saturated up to the surface. Thus, suction in the unsaturated zone is not considered, which is a pessimistic hypothesis for stability calculations, in particular in the lower part of the slide, in which the groundwater level before drainage is around 10 m (Fig. 7).

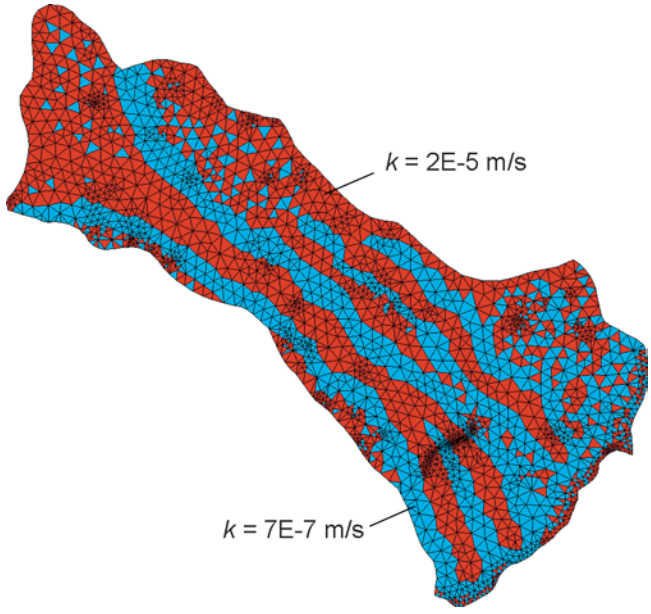

Fig. 9 Permeability field and values at finite elements layers 6 and 7 (near the main sliding surface)

Global model

At the landslide global scale, local heterogeneities (10 m wide) are not considered in the model and are replaced by a coarser system of channels (Fig. 9). This schematization, imposed by the calibration of the model, does not underestimate the connectivity of the real structures; consequently, the results must be read only at the landside scale and not at a local scale. Permeable channels are interrupted before their exit at the SE (Grande-Eau River) in order to avoid a too-fast emptying of the hydrogeological system. This configuration allows a fast balancing of pressures (transfer time) in the channels rather than a fast velocity field (transit time).

The model includes 12 finite element layers; layers 1–5 represent the active landslide (k=1×10^{-7} m/s), layers 6 and 7 represent the zone of the slip surface (Fig. 9), layers 8–11 represent the stabilised landslide ($k = 7 \times 10^{-7}$ m/s), whereas layer 12 includes the alluvium zone due to the Grande-Eau River at its lower part ($k = 1.5 \times 10^{-5}$ m/s)

Interpretation of pumping tests by means of analytical and numerical techniques suggests that except at the top of the aquifer, heterogeneities are captive. Indeed, the best specific storage coefficient S_s issued from calibration is 1×10^{-4} (m^{-1}), which expresses a fast response of the pressure field to temporal variations of the boundary conditions.

The simulation period ranges from August 1993 until December 1995, which corresponds to a well-monitored crisis episode. Flux boundary conditions on the border of the mesh change each day according to the weighting process described in the paragraph concerning infiltration conditions. An additional weighting is performed on these values according to the segment of border, so as to consider the area of substratum feeding this segment (17 border segments are distinguished). These conditions extend to the whole model thickness. At the top of layer 1, i.e. near the surface, an additional flux on all its area represents the direct infiltration, also changing daily and computed according to the weighting process (Fig. 10). Head boundary conditions concern

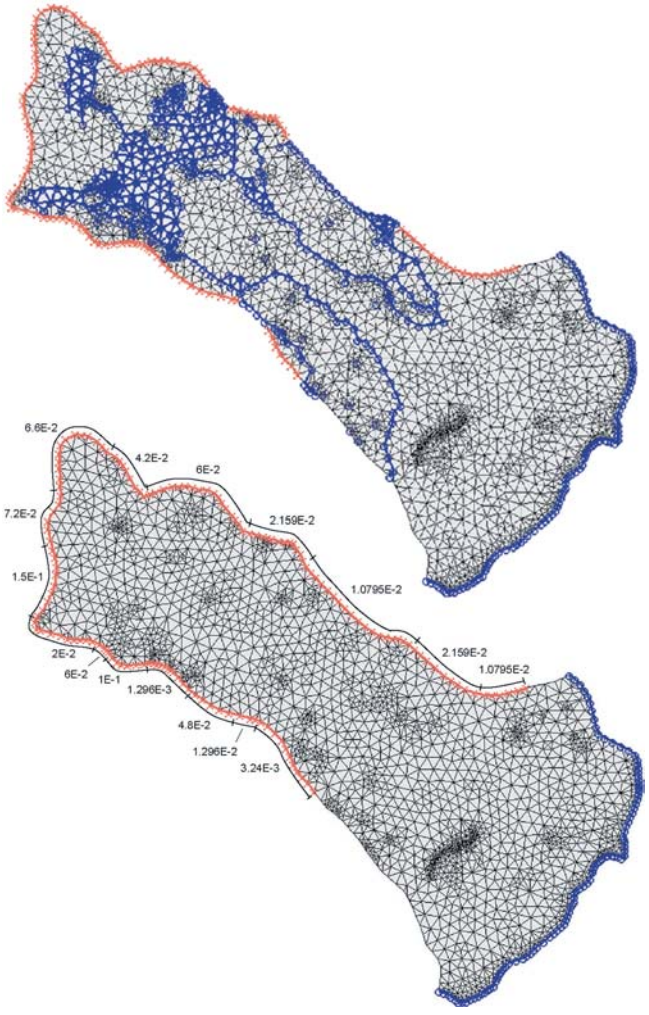

Fig. 10 Boundary conditions at node layer 1(*top*) and 2–9 (*bottom*). *Orange* flux boundary conditions. *Blue* hydraulic head conditions. At layers 10 to bottom of layer 12, conditions are identical to layers 2–9, except that head conditions are removed along the Grande-Eau River. The values at the perimeter of the slide are coefficients by which the net infiltration is multiplied in order to compute the lateral influx, taking the external drainage area and the geological conditions into account

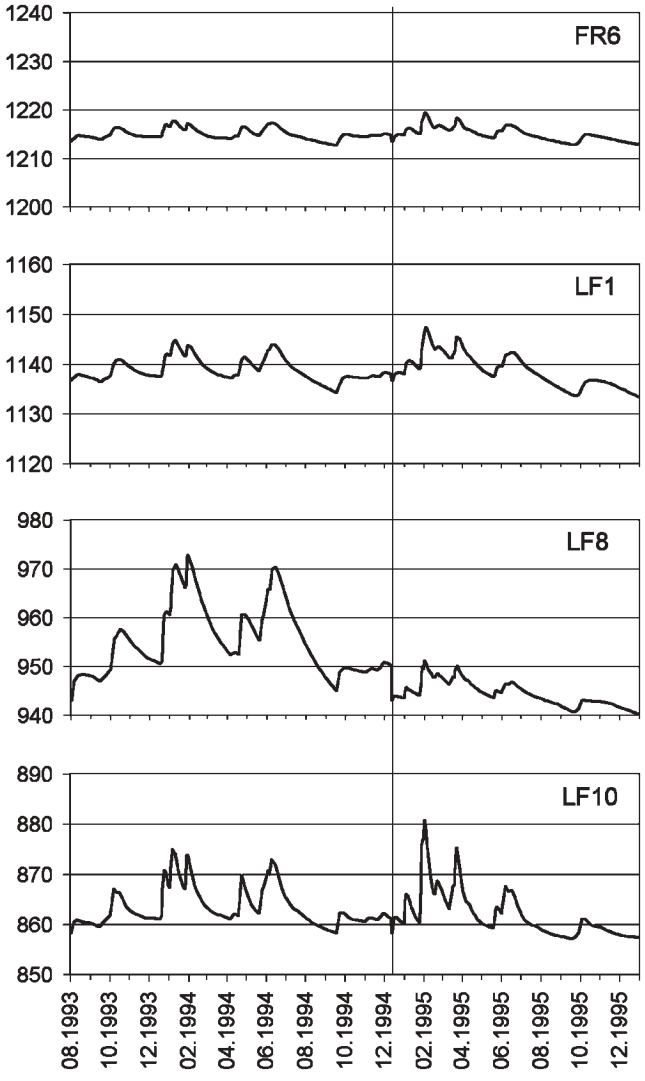

Fig. 11 Computed hydraulic head (m a.s.l) in some piezometers at the main slip surface level. Piezometer location is shown on Fig. 6. *Vertical line* commissioning of the pumping platform

the Grande-Eau River and springs of the uphill part of the surface (see paragraph concerning the outlets). All head boundary conditions at the top of layer 1 are set to $h=z$ (m), i.e. zero pressure. For layers 2–9, heads along the Grande-Eau are set to $h=z$ at the surface, i.e. equipotentials are vertical there. The fact to stop head boundary conditions at layer 9 along the Grande-Eau is somewhat arbitrary, leading to a satisfactory calibration of the model. This tuning is very sensitive on the result since it means to open more or less the main outlet of the system.

Since December 1994, the pumping platform is represented by adding constant head conditions at each of the 21 wells.

The major modelling results on a period of 883 days show that, in accordance with observations (technical reports by Norbert S.A. and de Cérenville S.A), daily hydraulic heads vary with time from some meters in the upper part of the landslide to some tens of meters downhill (Fig. 11). The magnitude of head fluctuations increases from the top of the landslide, reaches a maximum approximately at El. 900 m a.s.l. and then decreases quickly approaching the fixed heads along the Grande-Eau River (see LF10 borehole). In December 1994, the commissioning of the pumping platform caused a more than 5-m drawdown in its area (e.g. LF8 borehole). From this date, head fluctuations are noticeably reduced whereas the high infiltrations during spring 1995 had an obvious effect in the other regions of the slide (LF1, LF10).

The global hydraulic budget (Fig. 12) shows that the peaks of outgoing flow in the Grande-Eau occur only a few days after the peaks of inflow.

Apart from the infiltration peaks, approximately two thirds of the inflow comes from the borders of the slide, the remaining third coming from surface infiltration. This proportion is clearly reversed during important precipitation or snowmelt episodes (e.g. January 1994). During these periods, the hydraulic budget is more chaotic since buffer effect of the flysch substratum is dominated by the unsmoothed surface infiltration signal. The order of magnitude of the total flows entering and leaving the

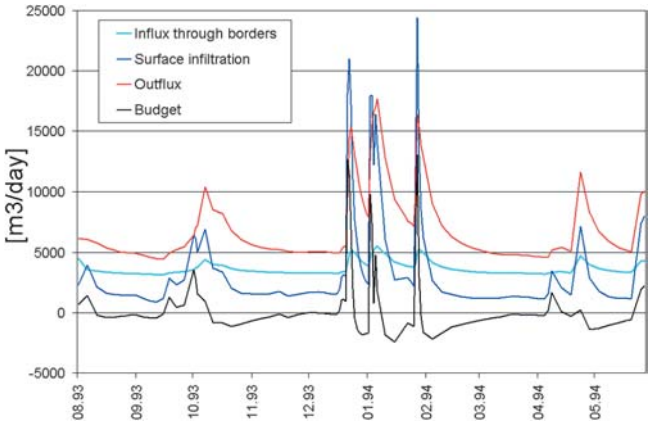

Fig. 12 Computed hydraulic budget between August 1993 and May 1994

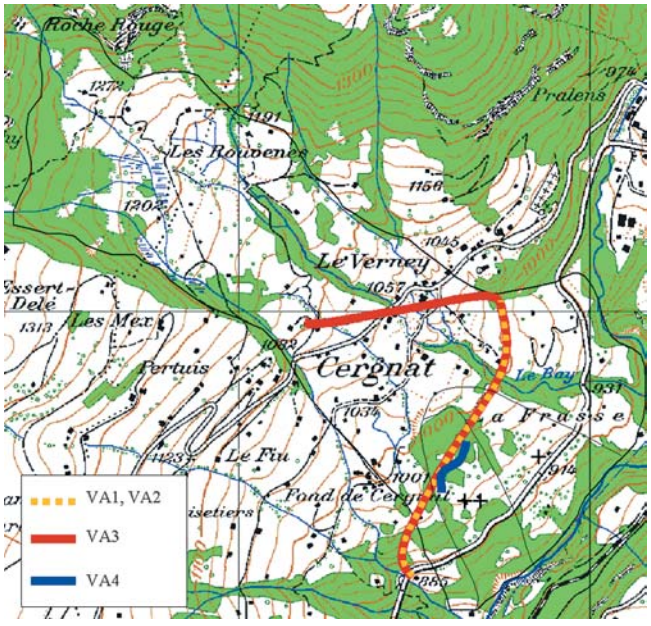

Fig. 13 Location of remediation designs

slide is 7,000 m³/day. From January 1995 on, the rates corresponding to the pumping platform range from 200 to 400 m³/day, which represents about 3% of the total flux in the slide (active plus stabilised).

Remediation designs

Starting from the base model, four remediation design schemes where considered by adding appropriate boundary conditions in the global model. All design schemes (Fig. 13) are located at the top of the active zones + and ++ so as to have a maximum impact on these zones while being protected from residual movements which could damage the works.

Design VA1 consists in a series of sub-vertical drains starting from a gallery that extends in the substratum over a length of 900 m throughout the whole landslide width. In the wells, hydraulic heads are set to the altitude of the main slip surface. Design VA2 has the same layout but the hydraulic head is set 10 m above the elevation of the main slip surface. Wells are drilled from the slope surface down to the slip surface. In VA1 solution, drains

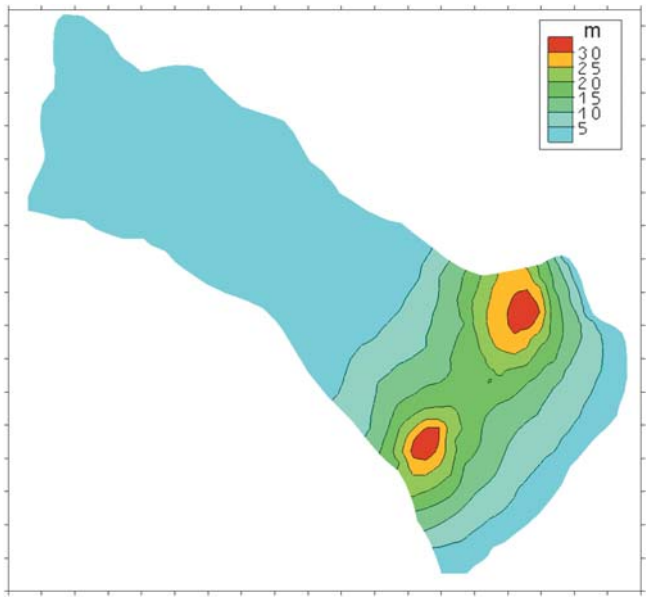

Fig. 14 Mean computed drawdown (m) at the main slip surface in design VA1. The high values are due to the slip surface depressions

starting from a gallery also drain the stabilised mass, thus causing global additional drawdown. In VA2, the wells, even deep, cannot drawdown water levels below the slip surface since in practice, residual movements impose the installation of the pumps above this surface. Otherwise, as shown by the existing 1995 platform, the pumps are progressively blocked in the drains and cannot be lifted and maintained anymore. Furthermore, the seepage face is estimated to be 10 m and thus reduces the head drawdown. VA3 is the U-shaped extension of VA1, with the upper branch protecting the lower one against possible residual movements. VA4 is the current state, i.e. the platform carried out in 1994 and commissioned in 1995, without additional wells. This variant was not examined further since geomechanical models showed that it would not have avoided the 1994 crisis.

Since the aquifer is captive (small specific storage coefficient), wells or drains have fast and long distance effects on the heads. This is why, according to the model, (Fig. 14) drawdown should be measurable at a distance of several hundreds of meters. In that sense, the captive nature of the aquifer, due to its high heterogeneity, is an aggravating factor since head fluctuations are higher and faster, but on the other hand, gives a much larger radius of influence to remediation wells or drains. Mean drained rates are 600 m³/day for design VA1, 500 m³/day for VA2 and 800 m³/day for VA3. They concern only a small percentage of the total flow in the model, i.e. 7,000 m³/day.

Local models

To estimate the optimum spacing between wells or drains, a sensitivity analysis is carried out with a schematic model in which connected heterogeneities are about 10-m wide (Fig. 15).

In this model, boundary conditions were set as follows:

- h varies cyclically between 200 m and 180 m in 5 days at y=1,000 m,
- h=100 m at y=0 m,

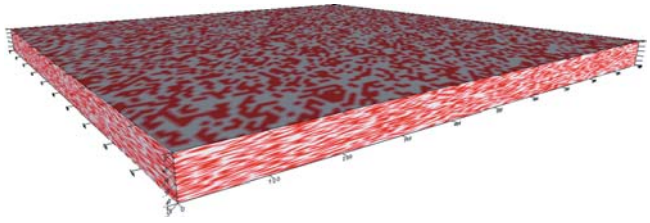

Fig. 15 Permeability field of the local models. Light grey: *k*=1E-7 m/s, red: *k*=1E-3 m/s. Model size is 1000 × 1000 × 40 m

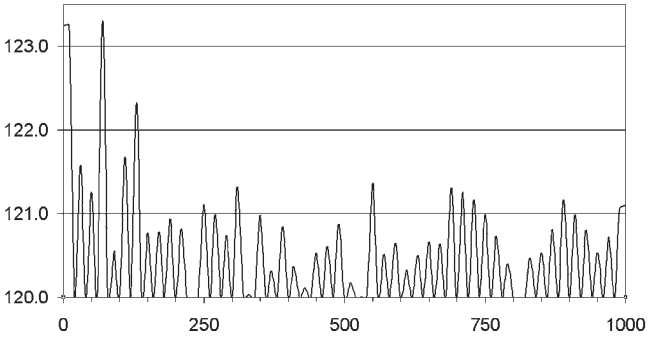

Fig. 16 Hydraulic head profile (m) at the top of the model at *y*=500 m at time *t*=1 day. Wells spacing = 20 m

- *h*=120 m at *y*=500 m at some nodes which corresponds to the wells,
- vertical sides, bottom and top are impervious,
- specific storage coefficient is assumed to be S_s=1E-4 (1/m).

Sensitivity analyses consist in varying the spacing between wells to 10, 20, 40, 80 and 120 m and checking the hydraulic head profile (Fig. 16).

The results show that a 10-m spacing is able to control the temporal head fluctuations between the wells within a range of some meters. This range increases quickly with the spacing. A 10-m spacing is thus considered as the most favourable mean value. In practice, wells or drains will have a larger spacing in a first construction stage and others will be added depending on the real encountered conditions.

Geomechanical modelling

This section illustrates the results of some geomechanical simulations of the effects of hydraulic condition changes on the mechanical behaviour of the landslide, in terms of displacements and effective stresses.

Mathematical formulation of the hydro-mechanical coupling

When the soil is considered as a two-phase saturated medium, interactions between the pore-water pressures and the mechanical behaviour of the solid skeleton may be obtained with a Biot-type mathematical formulation (Biot 1956). In such an approach, the mass and momentum of the fluid and solid phases are conserved. A thermodynamic description of the general form of the field equations is given in Laloui et al. (2003). The mass conservation equation of the soil is described by:

$$\frac{\partial tp}{Q} + \mathrm{div}\,\partial \mathbf{tu}_{rf} + \mathrm{div}\,\partial \mathbf{tus} = \mathbf{0} \qquad (1)$$

Q is an expression of the soil compressibility:

$$Q = \frac{1}{[n\,\beta_f + (1-n)\beta_s]} \qquad (2)$$

β_s and β_f are respectively the solid skeleton and fluid compressibilities, n is the porosity.

The velocity vector of the fluid infiltration $\partial_t \mathbf{u}_{rf}$ links the absolute velocities of the fluid, ∂tuf, and of the solid skeleton, $\partial_t \mathbf{u}_s$, by:

$$\partial tu_{rf} = n(\partial tu_f - \partial tu_s) \qquad (3)$$

Darcy's law is then introduced to link the infiltration velocity with the hydraulic head:

$$u_{rf} = -K\,\mathrm{grad}\,(\mathrm{p} + \rho_f \mathrm{gx}) \qquad (4)$$

where **K** is the tensor of the intrinsic soil permeability. It is a function of the pore size (porosity). p is the pore water pressure, ρ_f the volumetric mass of the fluid, **g** the vector of the acceleration due to gravity and **x** the position vector. Thus, the mass conservation is expressed by:

$$\mathrm{div}\,\partial \mathrm{tus} = \mathrm{div}[\mathrm{K}\,\mathrm{grad}(\mathrm{p} + \rho_f \mathrm{gx})] - \frac{\partial \mathrm{tp}}{\mathrm{Q}} \qquad (5)$$

As it can be seen, the temporal variation of the solid displacement (left side term) may be modified even by the Darcy's flow (first right side term) or/and the pore water-pressure variation (second right term).

The soil equilibrium equation is given by:

$$\mathrm{DIV}\,\sigma + \rho_{sat}\,\mathrm{g} = \mathrm{o} \qquad (6)$$

where σ is the total (Cauchy) stress tensor with tensile stresses taken as positive, and ρ_{sat} the total average mass density $\{= n\rho_f + (1-n)\rho s\}$, with ρ_s the mass density of the solid skeleton.

The capital divergence operator is defined as:

$$\{\mathrm{DIV}\,\sigma\}_{ij} = \Sigma_{ij}\partial_j \sigma_{ij} \qquad (i, j = 1, 3)$$

The behaviour of the solid matrix is assumed to be governed by Terzaghi's concept of effective stress given by:

$$\sigma = \sigma' - p\delta \qquad (7)$$

with σ' the effective stress tensor and δ the Kroenecker's operator. In the small strain approach adopted here, the effective stress tensor may be expressed in terms of the total strain tensor ε and the elasto-plastic constitutive tensor **D**; thus the momentum conservation equation takes the form:

$$\mathrm{DIV}\{\mathrm{D} : \varepsilon(\mathrm{u_s})\} = \mathrm{grad}\,p - \rho_{sat}\,\mathrm{g} \qquad (8)$$

Equations (5) and (8) compose then the two field equations with two unknowns ($\mathbf{u}_s$, p).

Constitutive modelling of the soil

In this study, two soil behavioural laws were used: a Mohr-Coulomb model (M-C) and the Hujeux elasto-plastic model (Hujeux EP) (Hujeux, 1985).

The Hujeux model incorporates the influence of confinement and stress path on the moduli, the consideration of the effects of overconsolidation as well as the influence of the void ratio on the behaviour (consideration of the critical state and dilatancy). It describes the soil behaviour using non-linear elasticity and four kinematic yielding mechanisms: one isotropic and three devia-

toric ones. These four mechanisms are activated during monotonous as well as cyclic (un-) loading. This enables to induce plastic strain even when the pore water pressure decreases in the landslide.

Each deviatoric mechanism has its own hardening parameters related to the distortion in the corresponding plane. All four mechanisms are coupled by the isotropic hardening parameter ε_v^p (volumetric plastic strain = $\Sigma_{k=1}^{4}(\varepsilon_v^p)_k$). The limit criterion is very close to that of Mohr-Coulomb. The plastic strain rate is defined through a plastic flow rule. Thus it is related to the yield surface, which depends on the stress state and on the internal variables (Modaressi and Laloui 1997).

Elasto-plastic formulations

Strains are partly elastic and partly plastic. The elastic strain rate is expressed as:

$$\dot{\varepsilon}_v^e = \frac{\dot{p}'}{K}$$

$$\dot{\varepsilon}_d^e = \frac{\dot{q}}{G}$$

where $\dot{\varepsilon}_v^e$ is the volumetric strain rate and $\dot{\varepsilon}_v^e$ the deviatoric strain rate; $\dot{q}$ is the deviatoric stress rate and $\dot{p}\prime$ the effective mean stress rate. K and G are the bulk and shear moduli, respectively. They depend from the mean effective stress:

$$K = K_{\text{ref}}\left(\frac{p'}{p_{\text{ref}}}\right)^{ne} \quad G = G_{\text{ref}}\left(\frac{p'}{p_{\text{ref}}}\right)^{ne}$$

where K_{ref} and G_{ref} are, respectively, the bulk and shear elastic moduli at a reference stress p_{ref} (the value of mean effective stress at which the elastic moduli are measured), and n_e is the non-linear elasticity exponent.

The deviatoric yield limit f_d can be represented by a Mohr-Coulomb criterion:

$$f\,d = q - p'\,Fr\sin\phi$$

with two hardening functions F and r. The volumetric hardening/softening function $F(p, \varepsilon_v^p)$ depends on the plastic volumetric strain:

$$F = 1 - b\left(\ln\frac{p'}{p_{co}} - \beta\varepsilon_v^p\right)$$

b is a numerical parameter, β the plastic compressibility modulus (the slope of the experimental line in the plastic volumetric strain versus critical pressure in a logarithmic scale) and p_{co} the critical state stress for the initial state. r induces the effect of the plastic deviatoric strain rate on the yield limit as a shear hardening. φ is the critical internal friction angle.

The isotropic yield limit is represented as:

$$f_i = p' - dp_{co}\exp^{\beta\varepsilon_v^p} r_{\text{init}}$$

where r_{init} corresponds to the size of the elastic domain. In the void ratio-Ln p' plane, d represents the distance between the perfectly plastic line and the isotropic consolidation line.

The plastic flow rule is given by:

$$\dot{\varepsilon}^p = \lambda \cdot \Psi$$

where λ is the plastic multiplier and Ψ is the direction of the strain increment.

Table 1 Material parameters of the landslide mass (see Table 2 for the slip surface – layer 3)

	Layer				
	1	2	4	5	6 (rock)
Young modulus (MPa)	80	80	100	100	(10,000)
Poisson ratio (–)	0.3	0.3	0.3	0.3	0.2
Internal friction angle (°)	30	30	33	33	45
Cohesion (MPa)	0.02	0.02	0.005	0.01	∞

Table 2 Material parameters of the slip surface of La Frasse landslide

Volumetric compressibility modulus	240 MPa
Shear modulus	111 MPa
Elastic non-linearity coefficient	0.3
Internal friction angle	25.5°
Plastic compressibility	19
Dilatancy angle	27.5°
Initial critical pressure	0.5 MPa

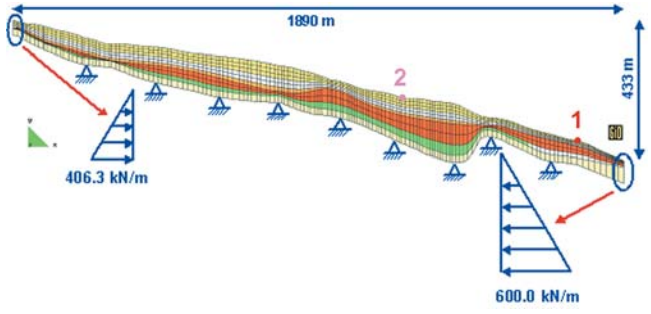

Fig. 17 2-D finite element mesh for the hydro-mechanical modelling

Finite element model

The two-dimensional mesh used for the geomechanical modelling is a cross-section through the centre of the landslide that passes by the points 1 and 2 (Figs. 2 and 17). This mesh includes 1694 nodes and 1530 4-node elements. On the basis of the results of the geotechnical investigations, six soil layers (see coloured zones in enlarged Fig. 18) were considered with different hydro-mechanical characteristics (Tables 1 and 2). In addition to the classic boundary conditions, equivalent loading forces were applied at the top and bottom of the landslide (Laloui et al. 2004) (Fig. 17). The loading force at the top is 406.3 kN/m and at the bottom it is 600 kN/m.

The initial state of stress is that induced by the soil weight at rest. The initial hydraulic conditions are those induced by the groundwater table.

Groundwater is recognized as the driving force of the landslide. Groundwater pressures resulting from the hydrogeological simulation (Fig. 18) are introduced as nodal forces in the geomechanical model. They vary over time at the edge of the second to last layer of the model.

The finite element geomechanical calculation was carried out through the *Gefdyn* code (Aubry et al. 1986). This program incorporates the mathematical hydro-mechanical formulation as well as the constitutive laws discussed in the previous section.

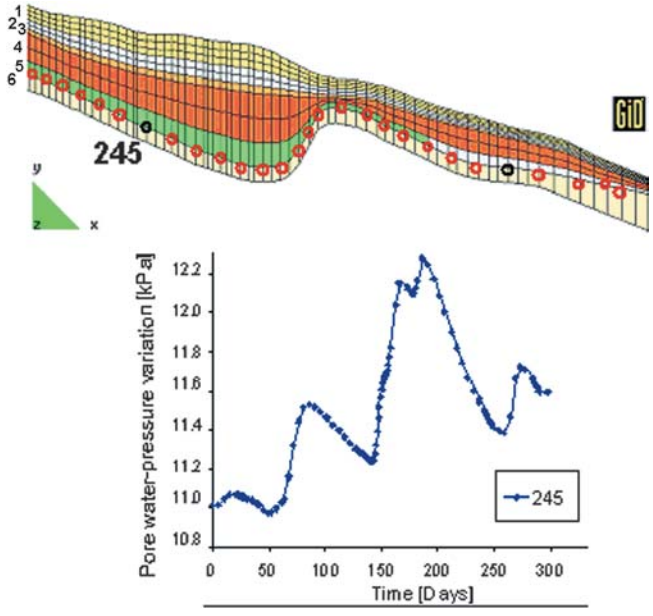

Fig. 18 Example on the way that the pore water pressures are applied (node 245): *circles* indicate the positions of nodes in which the pore water variation with time is imposed. The top cross section is a detail of Fig. 17

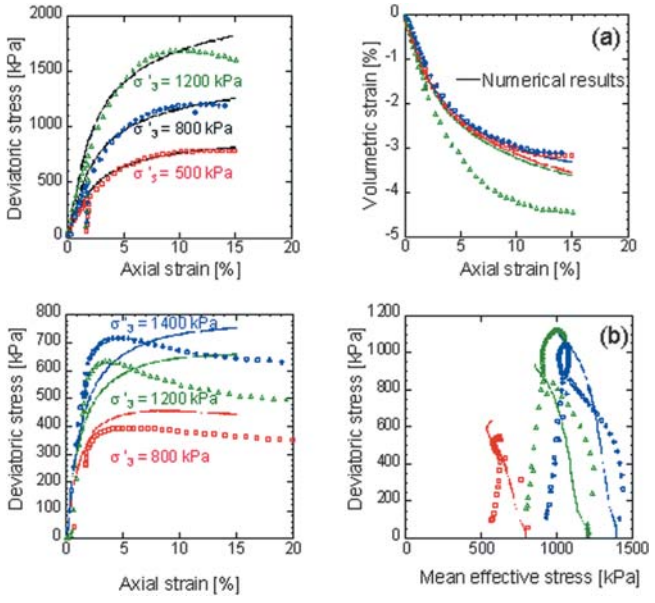

Fig. 19 Numerical simulation and experimental results of triaxial shear tests for three confining effective stresses: **a** Back-prediction of drained tests and **b** Prediction of undrained tests (continuous plots and symbol plots refer to numerical simulations and experimental data, respectively)

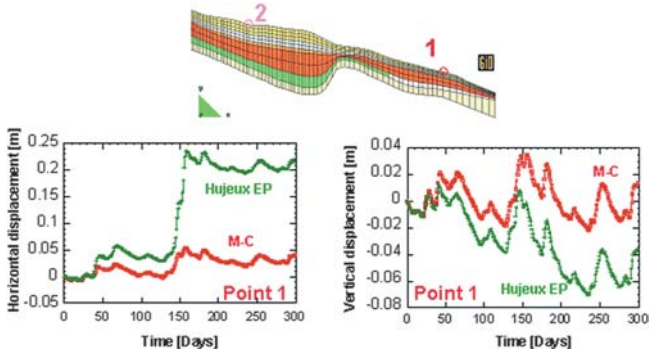

Fig. 20 Numerical simulation of the landslide displacements using two constitutive models for the slide layer: Hujeux elasto-plastic and Mohr-Coulomb (M-C) constitutive models

Hydro-mechanical parameters of the slip surface

On the basis of the geotechnical investigations, it was decided to consider that all the soil layers apart from the slip surface (layer located between 35 and 45 m depth in the lower part of the slide) would follow a Mohr-Coulomb-type law. The behaviour of the slip surface was carefully considered and two constitutive models were adopted: the Mohr-Coulomb and the Hujeux cyclic elasto-plastic model. In order to calibrate the model parameters, laboratory tests including drained and undrained triaxial tests were carried out on the samples obtained from two additional boreholes drilled in 2002

Figure 19 presents the numerical simulations of triaxial tests with the Hujeux elasto-plastic model, compared to the experimental results. The drained triaxial tests were used for the determination of the model parameters (Fig. 19a). The samples seem to exhibit a normally consolidated behaviour with a plateau for the shear strength and the volume compression. The main model parameters obtained from these tests for the slip surface are indicated in Table 2 (Hujeux 1985).

Using these model parameters numerical predictions were carried out for the undrained triaxial tests with three confining stresses (500, 800 and 1,200 kPa). With respect to the previous experimental tests, the main difference in the stress paths lies in the fact that the drainage is not allowed now. In this case a coupled hydro-mechanical process is considered. The model predictions (Fig. 19b) are of a very good quality for the shear strength as well as for the excess pore water pressure (difference between the mean effective stress and the total stress applied to the sample). However, the soil samples at confining pressures of 1,200 and 1,400 kPa seem to show a slight overconsolidation.

From the spatial discretisation, Eqs 5 and 8 are resolved at each Gauss point. For each element, the stress-displacement relation is solved. The material parameters obtained at the laboratory scale (triaxial samples) are supposed to be representative of the material behaviour at the in-situ scale.

Effects of the constitutive model on the numerical simulation of the landslide

In order to evaluate the improvements resulting from the use of a sophisticated model for the shear surface, Fig. 20 presents the numerical results obtained with the Hujeux-type elasto-plastic model in comparison to those obtained with the use of the Mohr-Coulomb model. The comparison is made for the crisis that the landslide underwent in 1994 over a period of 300 days. The pore pressures introduced in the model during this period are those obtained from the hydrogeological model.

The horizontal and vertical numerical displacements at point 1 at the surface of La Frasse landslide obtained with the Hujeux elasto-plastic model are closer to the observed acceleration than

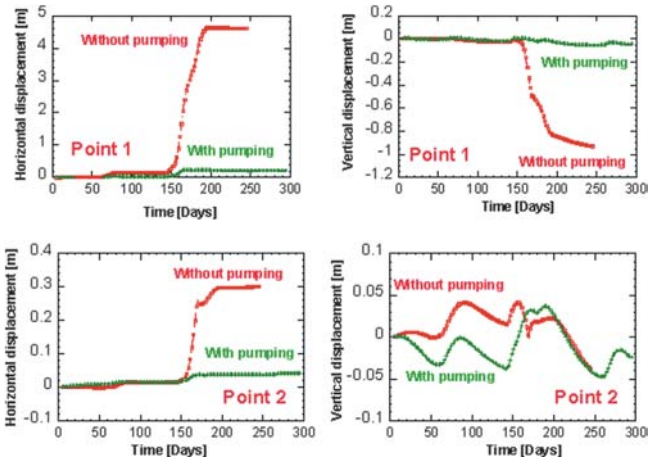

Fig. 21 Pumping effects on the landslide displacements. The maximum observed movement is around 2.6 m

those obtained with the Mohr-Coulomb model. This difference results from the way in which the progressive soil yielding (hardening) is taken into account in the formulation of the two constitutive models. Based on the considered geomechanical characteristics, the main modelled shear displacements occur at the slip surface, as it is observed in the inclinometer readings.

Influence of drainage pumping

One of the remediation solutions aimed at reducing the landslide movements is the installation of drainage pumping (see Fig. 13). Comparison between the displacement fields with and without pumping (or draining through a gallery in the bedrock) for the case of the 1994 crisis is shown in Fig. 21. These results clearly show that this solution strongly modifies the intensity of the horizontal and vertical landslide displacements reducing the movements down to 5% of the values modelled during the whole crisis, for a point near the drainage curtain. Despite of the fact that the drainage boreholes are put along a simple line, their effect is quite marked even at point 2, located some 300 m upstream from the drainage curtain.

The total displacements near to point 1, monitored during the 1994 crisis, which reaches some 2.6 m is thus quiet similar to the 2-D modelling results. The correspondence is even better with the 3-D modelling carried out by the sub-contractor GEOMOD S.A (Commend et al. 2004).

Conclusions

The integration of the heterogeneous character of the landslide mass in the hydrogeological and geomechanical modelling of the La Frasse landslide has supplied a significant contribution to increase the reliability of the computed movements during crises. However, it has to be kept in mind that the size of the considered heterogeneities is fairly large, so that the results have a meaning at the global scale of the slide, and not at a local scale. For this reason, the recommended borehole spacing is limited to about 10 m, even though it appears that the drawdown caused by the planned drainage system may extend efficiently to more than 200 m away.

The proposed drainage design scheme with boreholes drilled from a deep gallery excavated in the bedrock can be completed by some surface drainage and correction works allowing a reduction of infiltration in the aquifer. However, these works have a reduced impact on the flow balance, as the total average inflow reaches some 80 l/s, whereas the flow of the Bonne-Eau River is approximately 1 l/s. Nevertheless, the reduction of direct infiltration from the surface of the slide contributes to decrease the more rapid unfavourable pressure fluctuations.

As far as the geomechanical modelling is concerned, the use of an advanced elasto-plastic constitutive model, i.e. the Hujeux model, may supply more appropriate results than classical models; its consideration is in particular meaningful in the modelling of the layer in which the major shear movements occur. The results obtained with conservative assumptions prove that a well-designed drainage scheme may provide a substantial stabilising effect during a crisis, although this type of work requires a regular maintenance programme; these results ensure the sustainability of the proposed scheme as the drains should not be sheared at the slip surface.

Acknowledgements

The authors express their thanks first for the financial support and critical discussion provided by the Office for Water, Soil and Sewage of the Canton of Vaud and by the Swiss Federal Office for Water and Geology for allowing the fulfillment of this fascinating research project. Then they wish to express their acknowledgements to all the private consultant partners for a positive collaboration, in particular to Geomod SA, which contributed in an essential way to the project by its 3D-modelling computations

References

Association technique Norbert, de Cérenville Géotechnique + EPFL pour l'étude du glissement de La Frasse (2004) Glissement de La Frasse, modélisation et étude de faisabilité, unpublished report

Aubry D, Chouvet D, Modaressi A, Modaressi H (1986) Gefdyn software—Logiciel d'analyse du comportement mécanique des sols par éléments finis avec prise en compte du couplage sol-eau-air. Ecole Centrale Paris

Biot MA (1956) General solutions of the equations of elasticity and consolidation for a porous material. J Appl Mech 78:91–96

Bonnard Ch. (1984) Determination of slow landslide activity by multidisciplinary measurements techniques. In: International symposium on field measurements in geomechanics, Zürich, Balkema edn, 1:619–638

Commend S, Geiser F, Tacher L (2004) 3D numerical modeling of a landslide in Switzerland. In: Proceedings of the International Symposium on Numerical Models in Geomechanics NUMOG IX, Ottawa, pp 595–601

Feflow groundwater modelling software, Wasy AG, Berlin

Hujeux JC (1985) Une loi de comportement pour le chargement cyclique des sols. Génie Parasismique, Edition V. Davidovici, presses de l'E.N.P.C., Paris

Jansson P-E, Karlberg L (2001) Coupled heat and mass transfer model for soil-plant-atmosphere systems. Royal Institute of Technology, Department of Civil and Environmental Engineering, Stockholm, 325 pp

Laloui L, Klubertanz G, Vulliet L (2003) Solid–liquid–air coupling in multiphase porous media. Int J Num Anal Methods Geomech 27(3):183–206

Laloui L, Tacher L, Moreni M, Bonnard C (2004) Hydro-mechanical modeling of crises of large landslides: application to the La Frasse landslide. In: Proceedings of the IX International Symposium on Landslides, Rio de Janeiro, Balkema edn, pp 1103–1110

Lugeon M, Paschoud E, Rothpletz F (1922) Rapport d'expertise sur le glissement des Frasses, Etat de Vaud, Département des Travaux Publics, Service des Routes

Modaressi H, Laloui L (1997) A thermo-viscoplastic constitutive model for clays. J Num Anal Methods Geomech 21:313–335

Norbert SA, de Cérenville SA (1979) Technical reports since 1979

Noverraz F, Bonnard Ch (1990) Technical note on the visit of La Frasse landslide. In: Proceedings of the Vth International Symposium on Landslides, Lausanne, Balkema edn, 3:1549–1554

Parriaux A, Lutz T, Tissières P (1987) Traçage au gouffre du Chevrier (Préalpes vaudoises) et méthodes d'identification de l'uranine à faible concentration. Bull Centre d'Hydrogéol l'Univ Neuchâtel 7

Prina E, Bonnard Ch, Vulliet L (2004) Vulnerability and risk assessment of a mountain road crossing landslides. Rivista Italiana Geotecnica XXXVIII(2):67–79

Vulliet L, Hutter K (1988) Continuum model for natural slopes in slow movements. Géotechnique 38(2):199–217

L. Tacher (✉) · A. Parriaux
Laboratory of Engineering and Environmental Geology (GEOLEP),
Institute of infrastructures, resources and environment,
Swiss Federal Institute of Technology Lausanne, EPFL- ICARE,
CH-1015 Lausanne, Switzerland
e-mail: laurent.tacher@epfl.ch
Tel.: +41-21-6932356
Fax: +41-21-6936330

C. Bonnard · L. Laloui
Laboratory of Soil Mechanics (LMS),
Institute of infrastructures, resources and environment,
Swiss Federal Institute of Technology Lausanne, EPFL- ICARE,
CH-1015 Lausanne, Switzerland